

Computational Evaluation of Frictional Force Changes in Three-Point and Three-Bracket Bending Models

S. A. H. A. Seman, M. F. Razali*, A. S. Mahmud, M. H. Hassan
School of Mechanical Engineering, Engineering Campus,
Universiti Sains Malaysia, 14300 Nibong Tebal, Pulau Pinang, Malaysia
*mefauzinizam@usm.my

ABSTRACT

NiTi arch wires are commonly used at the initial stage of orthodontic treatment, due to their superelastic and biocompatibility properties. Numerous bending models have been considered to anticipate the mechanical responses of the superelastic NiTi wire in the oral environment. It is known that the magnitude of bending force exerted by the NiTi wire is relatively influenced by the magnitude of friction generated at the wire-support interfaces. These data on the variability of friction magnitude for various bending models, however, are very limited in the literature. This study investigated the magnitude of frictional force generated in different bending models through the numerical method. The frictional force in a three-point and a three-bracket model was quantified from the force difference, measured when the wire was deflected in friction and frictionless conditions. Overall, the frictional force magnitude gradually increased as the wire further pressing the support surface at higher deflection. The highest frictional force was recorded when the bracket support was considered, with values of 2.01 N during loading and 1.61 N during unloading. These loading and unloading frictional forces were significantly reduced to 0.25 N as soon as the point support was considered. The high frictional force generated in the bracket model transformed the constant force-deflection trend of superelastic NiTi wire into a gradient force.

Keywords: Superelastic; Orthodontic; Bending; Friction; Gradient Force

Introduction

Orthodontic treatment is typically performed using fixed appliance therapy because it facilitates correct alignment of the tooth [1]. The process of moving the malposed tooth can be categorized into three stages. The first stage aims to align and level the teeth, the second stage aims to correct the bite between the top and bottom teeth and the last stage aims to minimize the gap between the teeth [2]. These stages of treatment are performed due to the bending recovery of the arch wire after it has been inserted into the bracket slot. When the arch wire seeks to restore its straight form over the process of therapy, the malposed tooth is pushed slowly in the direction of bending recovery, thus induces tooth movement.

The force needed to initiate tooth movement originates from the spring-back ability of the bent arch wire. Several arch wire materials are available to generate this force, ranging from stainless steel and nickel-titanium to cobalt-chromium and beta-titanium [3]. Owing to its potential to exert light and constant force at a large deflection range, superelastic NiTi wires are often used for levelling and aligning purposes. This unique constant force mechanic is manifested from its thermo-elastic martensitic transformation, which can be defined as a first order displacive non-diffusion mechanism [4].

Superelastic NiTi wire shows the force of bending over a force plateau when loading and unloading in a three-point model [5]. In truth, this constant force behaviour is a portion of interest since it represents the capacity of NiTi wire to provide consistent and light force to the dentition. As the classic bending model ignored the function of bracket engagement, the tendency for manufacturers to advertise their arch wire products centered on the force-deflection curves obtained from three-point bending experiments was found to be incorrect. Whenever the dental bracket is considered, arch wire unloading inside the bracket configuration induces sliding friction at wire-bracket interfaces. As a result, several studies documented a gradient force-deflection behaviour of NiTi wires in the bracket model when bending at high deflection (over 2.0 mm) [6–9]. These gradient force plateaus are believed to be created by the variation in the frictional force intensity, as the wire deflected further at large deflection [8, 10]. However, due to the limitation of the current experimental setup, no research work has been carried out to measure the friction-deflection data from the bending test.

In this study, a numerical approach was utilized to determine the strength of frictional force encountered by superelastic NiTi wire while bent under various models. For this purpose, two finite-element models were developed, denoting the bending of superelastic NiTi wire under three-point and three-bracket configurations. The three-point model was used in this work as a reference, due to the current trend of wire manufacturers to record

the NiTi wire force using this setup. The frictional force of both models was obtained from bending force differences measured in friction and frictionless bending condition. This numerical approach allows the quantification of frictional force differences in both bending models, as well as foreseeing its impact on the flexural nature of the superelastic NiTi arch wire.

Methodology

A commercial finite-element analysis package, Abaqus/CAE v6.12.2 was used to develop two finite-element bending models. The assembly of the NiTi wire in the three-bracket and the three-point models are shown in Figure 1(a) and Figure 1(b), respectively. Both bending models considered asymmetrical configuration of wire bending. The three-bracket model was developed by considering the instances of a single round arch wire and three dental brackets. An instance of 0.4-mm diameter straight wire was modelled from 72,144 linear hexahedral C3D8R elements. The wire was set to be 30 mm in length. The global element size was set to 0.060 mm, with a finer element size of 0.035 defined at the potential region of contact between the wire and the bracket.

As shown in Figure 1(a), the bracket instance was created by placing two bracket halves in opposite directions. The bracket halves were distanced by 0.46 mm to mimic the slot height of the common dental bracket. The bracket instance was created from a bilinear rigid quadrilateral element (R3D4). Every bracket was distanced from its midpoint by 7.5 mm in between. The two halves of the bracket were assigned to a single reference point to allow the boundary condition set at this point to be applied to the whole bracket instance. The wire bending was accomplished by vertically displacing the centre bracket by 3.0 mm, while the adjacent brackets were limited from moving by using the 'encastre' option.

The bending (loading) and recovery (unloading) of the wire were achieved by moving the central bracket in negative and positive y-direction, respectively. The displacement rate of the central bracket was set to 0.016 mm/s. The model's temperature was set to stay constant at 26 °C throughout the bending duration. The forces-deflection curve of the bent superelastic NiTi arch wire was obtained from the vertical reaction force and displacement data of the central bracket.

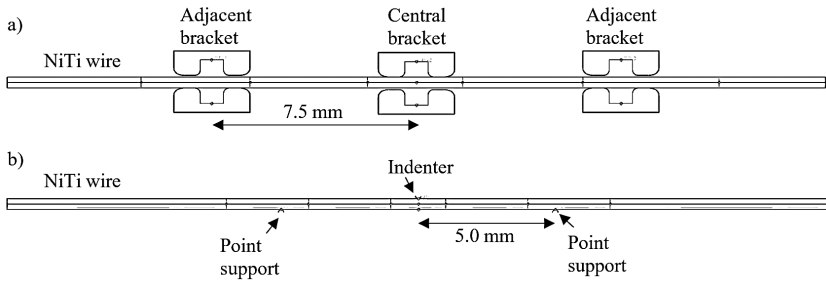


Figure 1: Engagement of NiTi wire in the: (a) three-bracket and (b) three-point model.

Simulations of wire bending were conducted under friction and frictionless settings, which were accomplished by changing the coefficient of contact friction at the wire-bracket interface. The friction coefficient for the friction case was set at 0.27 and this value was obtained from the norm friction coefficient reported for the contact of NiTi wire and stainless-steel bracket [11]. Hence, the force data obtained from this condition is contributed from the summation of bending and frictional force. Meanwhile, in the frictionless situation, a minimum friction coefficient of 0.01 was specified to preserve the numerical solution's stabilization. Since this coefficient value is very tiny, it is assumed that the force-deflection result produced from this setting will only feature the actual bending force of the NiTi wire.

The three-point bending model was developed by considering a single NiTi wire placed on two-fixed supports distanced at 10 mm. As seen in Figure 1(b), a rigid semi-circle element of 0.1 mm radius was depicted as the supports and the indenter. Similar to the three-bracket model, the appropriate element form, mesh size, contact properties, and analysis steps were set, except that the supports were modified to point support distanced at 5.0 mm in between. The supports and indenter were allocated to their point of reference. Only the indenter was set to travel in the y-direction, while the motion was limited in all directions on the neighbouring supports (where U_x , U_y , and U_z are set to 0). The overall deflection was set at 3.0 mm deflection and the bending was done at a displacement rate of 0.016 mm/s by traveling the indenter vertically downwards and then upwards.

A user material subroutine based on Aurrichio and Taylor's algorithms [11], was utilized to anticipate the superelasticity response of the NiTi arch wire. The material subroutine was enabled by providing the 13 material parameters needed in the material property section. The value of each parameter is listed in Table 1. These material data were measured against uniaxial tensile and bending tests from our previous experimental study [12].

Table 1: Mechanical properties and superelastic behavior of NiTi arch wire [12]

Parameter	Description	Value (unit)
E_A	Austenite elasticity	44 (GPa)
(ν_A)	Austenite Poisson's ratio	0.33
E_M	Martensite elasticity	23 (GPa)
(ν_M)	Martensite Poisson's ratio	0.33
(ϵ_L)	Transformation strain	0.06
$(\delta\sigma/\delta T)_L$	Stress rate during loading	6.7 (MPa/°C)
σ_{SL}	Start of transformation loading	377 (MPa)
σ_{EL}	End of transformation loading	430 (MPa)
T_0	Reference temperature	26 (°C)
$(\delta\sigma/\delta T)_U$	Stress rate during unloading	6.7 (MPa/°C)
σ_{SU}	Start of transformation unloading	200 (MPa)
σ_{EU}	End of transformation unloading	140 (MPa)
σ_{SCL}	Start of transformation stress in compression	452 (MPa)

Results

The force-deflection curves of NiTi wire generated from the three-point and three-bracket models are shown in Figure 2. The arch wire exhibited the loading and unloading curves over a force plateau in the three-point model. The formation of the force plateau implied that the deformation of the wire was commenced under superelastic behaviour. On the opposite, these loading and unloading curves in the presence of brackets have turned into a positive and negative gradient slope, respectively.

The gradient bending force pattern was formed due to the gradual increase in friction intensity as the wire curvature hardly pressed the bracket corners at large deflection. Meanwhile, the intense friction created at the beginning of the bending recovery greatly reduced the unloading force, before this force rose progressively following a reduction in wire deflection. It is important to notice that the load force from the bracket model surpassed the force from the point model by 2.5 times at a 3.0-mm deflection. This observation is supported by the previous finding in [13], who reported up to 40 times increment of wire loading forces upon replacing the point supports of the bending setup with the dental brackets.

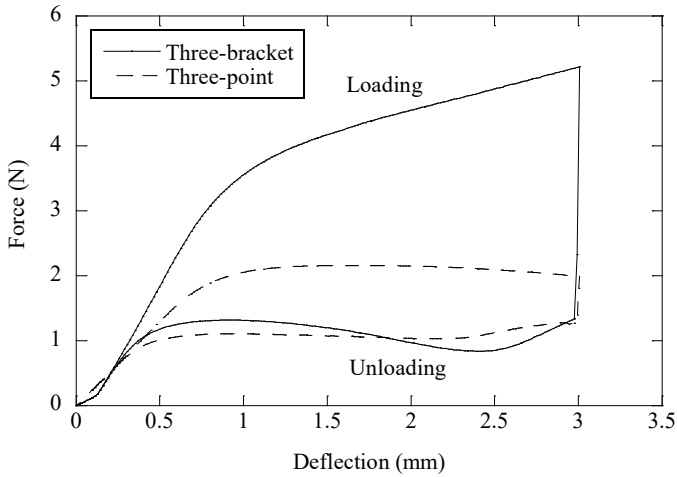


Figure 2: Force-deflection curves of NiTi arch wire undergoing bending in the three-point and three-bracket model.

Figure 3(a) and Figure 3(b) portray the force-deflection behaviours of superelastic NiTi wire under frictionless and friction conditions when using three-point and three-bracket models, respectively. The variations in force level between the two curves were defined as f_{loading} and $f_{\text{unloading}}$, showing, respectively, the extent of the friction the arch wire encountered during the loading and unloading cycles. The wire from the three-point model exhibited a typical force-deflection behaviour in both friction and frictionless conditions, indicated by the presence of the force plateaus. Due to the lack of a friction factor in the frictionless case, the loading of the wire from 1.0 mm to 3.0 mm was accompanied by a natural reduction of the force. This force reduction pattern relates to the reduction of the flexural stiffness of the wire due to the addition of wire length involved during the bend. As the input from friction was ideally eliminated during frictionless bending, the wire deformation alone contributes to the registered bending force. Fortunately, this pattern of force reduction does not occur in the situation of friction, as the loading and unloading force is steadily increased and delayed by progress in friction intensity. Note that at 3.0 mm, friction raised the loading force from 1.74 N to 1.99 N and decreased the unloading force from 1.51 N to 1.26 N.

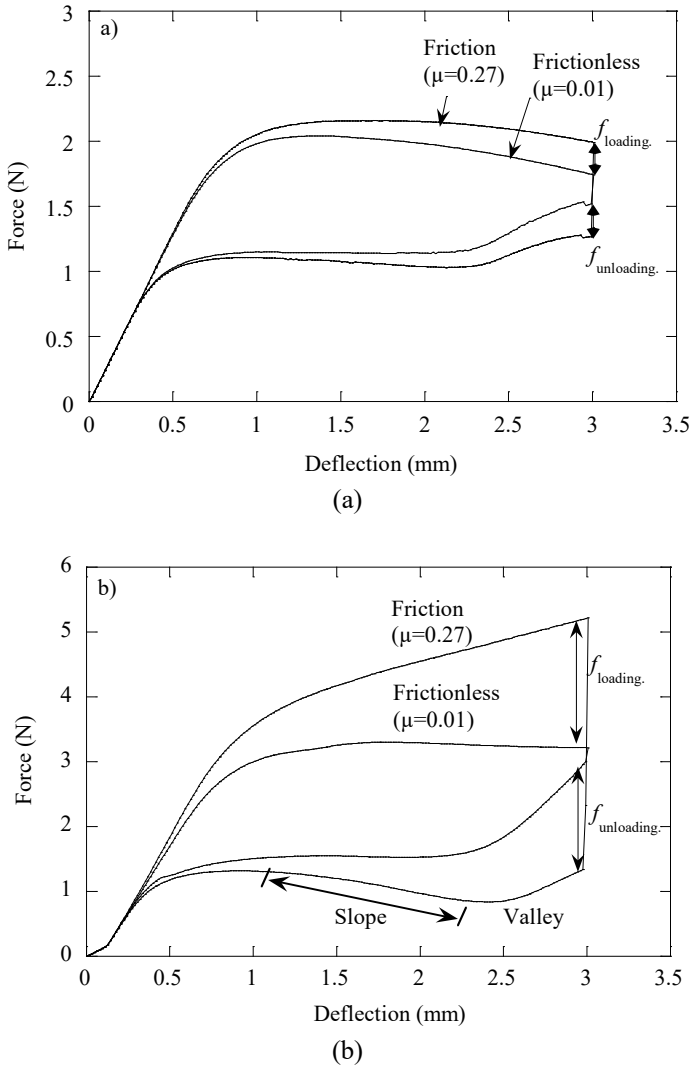
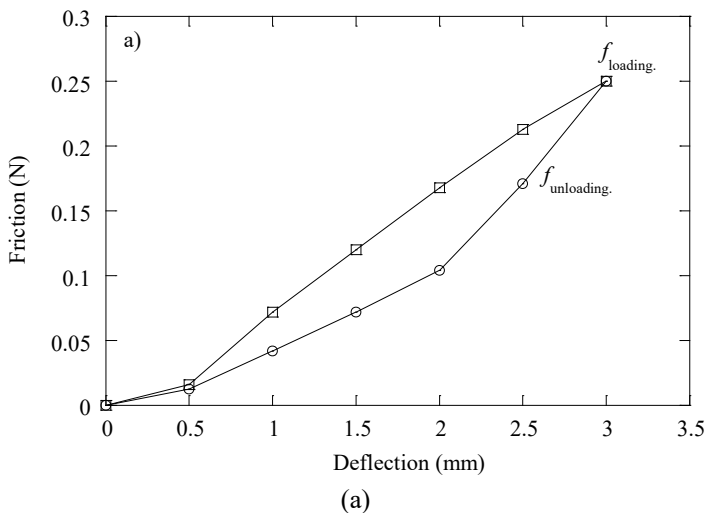


Figure 3: Force-deflection curves of NiTi wires undergoing bending in frictionless and friction conditions using: (a) three-point bending model and (b) three-bracket bending model.

On the other hand, a considerable effect of frictional force was observed on the NiTi wire's bending response in the bracket model. As seen in Figure 3(b), the consideration of the friction factor in the bracket model

caused the wire to deliver the loading and unloading force over a positive and negative slope curve. For example, the friction intensity generated at 3.0 mm deflection significantly increased the loading force from 3.22 N to 5.21 N. Contrarily, at the same wire deflection, friction delayed the unloading force from 2.95 N to 1.34 N. All in all, this frequent change of force magnitude provides an insight into the fact that NiTi wire no longer exerts a constant and light force on the dentition when the bracket model was utilized during orthodontic treatment.

Figure 4(a) and Figure 4(b) display the differences in friction magnitude experienced by the NiTi wire during bending in the three-point and three-bracket models. In short, friction increased gradually as a function of wire deflection, and higher friction values were registered at the loading cycle than during unloading. Over the 3.0 mm deflection, the friction values gradually increased to 0.25 N and 2.01 N when the point and bracket model were considered, respectively. It is worth noting that in the presence of the bracket, greater friction was produced, given that the curvature of the wire was restricted within the bracket slot. For instance, during unloading at 3.0 mm, the wire in the bracket model experienced about 1.6 N friction, which is 6.4 times higher than the friction recorded in the point model. This explains the sudden force reduction (force valley) at the onset of the bending recovery, as shown in Figure 3(b). This force valley was not observed on the point model's unloading curve, as the magnitude of friction is very small at about 0.25 N.



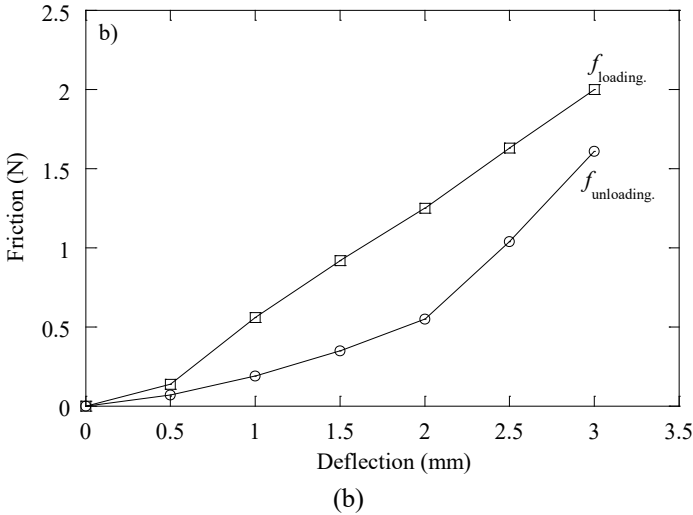


Figure 4: Variation of friction magnitude in the (a) three-point and (b) three-bracket bending model.

The rise in the strength of friction with respect to the deflection added can be related to the degree of the deformation of the wire at the edge of the bracket. Figure 5 presents the progress of the local stress, σ along the wire length throughout the 3.0 mm bracket displacement. In total, there are four deformed regions were spotted on the wire: one at the edge of each adjacent bracket and the other two at both edges of the central bracket. The blue and red color regions represent the compression and tension area of the wire curvature, respectively. Following the linear strain profile concept, the stress was observed to increase from the core to the outer region of the wire.

The stress contour reflects the rise in the principal stress value from the middle line region to the outermost tensioned region. It is seen that as the wire being deflected from 1.0 mm to 3.0 mm, the principal stress of the wire curvature near the bracket corners has increased from 399 MPa to 678 MPa. To preserve the rise of wire curvature at higher deflections, a larger pinching force must be applied at the neighbouring bracket surfaces, resulting in an increased degree of friction. In general, this stress distribution obtained from the finite-element model corresponds favourably to the findings stated in [14].

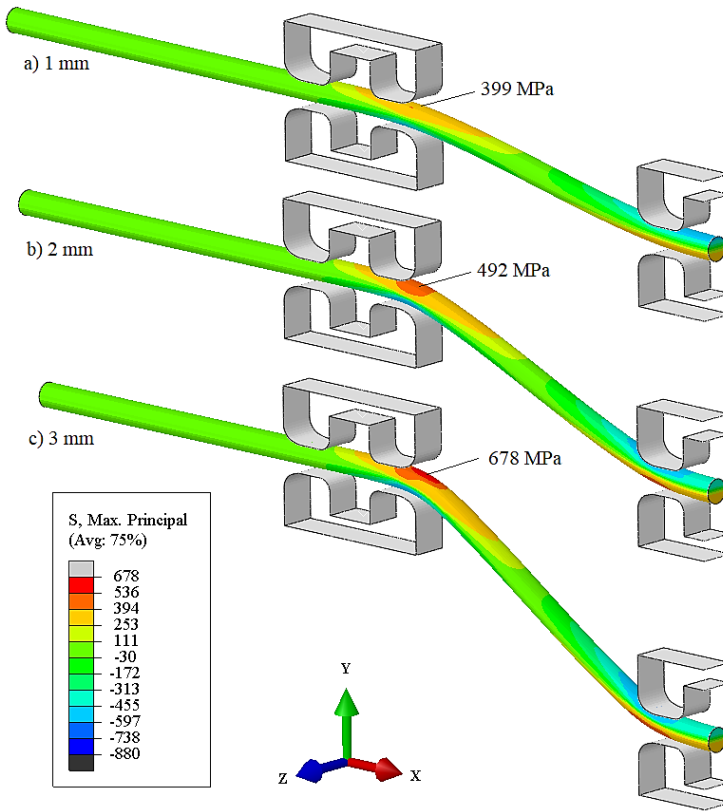


Figure 5: A view cut of principal stress contour of superelastic NiTi wire in the three-bracket model.

On the other hand, Figure 6 shows the deformation behaviour of the superelastic NiTi wire when bend in a three-point model. It is seen that the wire deformation was concentrated only at the middle region, where the indenter was displaced. The inset shows that the maximum principal stress at the wire curvature greatly increased from 398 MPa to 870 MPa as the wire was deflected from 1.0 mm to 3.0 mm. During the bending course, a less pinching force can be expected to be exerted on the support surfaces as no wire deformation has been observed near the support area. Consequently, during the sliding motion, the wire encountered less resistance, resulting in lesser changes in the pattern of force-deflection as seen in Figure 3(a).

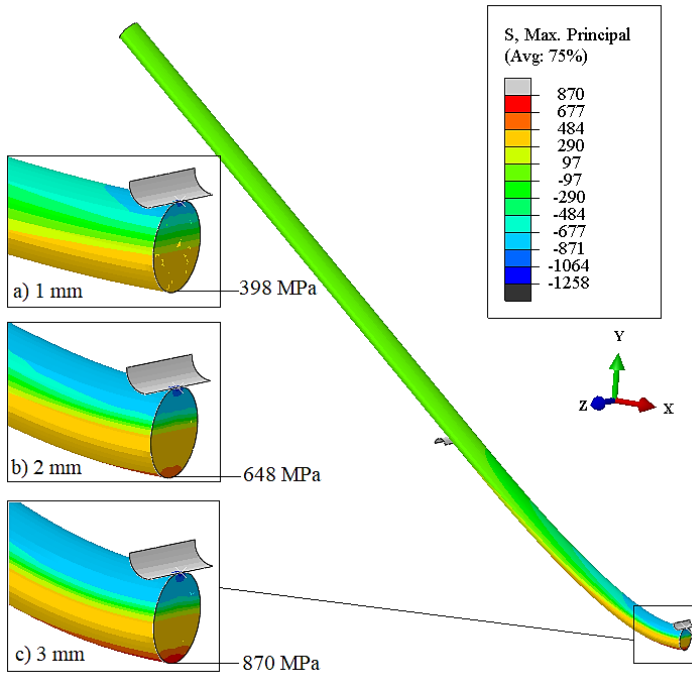


Figure 6: A view cut of principal stress contour of superelastic NiTi wire in the three-point model.

Discussion

In this computational study, the magnitude of frictional force encountered by NiTi arch wire during bending in the three-point and three-bracket model were measured by using the numerical approach. The numerical model considered the standard case of tooth levelling treatment, considering the engagement of 0.4 mm round NiTi wire inside the 0.46 mm-slot height bracket. The numerical approach provides advantages in terms of having room for adjustment of the friction coefficient at wire-bracket interfaces, as well as in predicting material responses in the simulated environment [15–17]. For each bending model, the frictional force was determined by measuring the difference in loading and unloading force exhibited by the wire during bending in frictionless and frictionless conditions. The friction data obtained in this study offers a clear insight into how the sliding friction

of the wire differs over various bending models, as well as the effects of friction on the force-deflection trend.

It should be remembered that the friction data obtained from the wire-bracket model are only relevant to the existing bracket configuration. If, for example, the same wire size is bent in a narrower inter-bracket setting, greater frictional force can be expected from Figure 4(b). This is because, due to the shortening of the wire length available between brackets, the wire is supposed to indent the bracket corner harder as the wire curvature getting wider. In addition, since the thermomechanical behaviour of NiTi wire is known to be very sensitive to temperature change [18, 19], the magnitude of friction is also expected to differ as soon as hot or cold intakes are consumed by the patient.

The key goal of orthodontic therapy is to accelerate tooth movement and produce as minimal pain as possible. An ideal wire-bracket arrangement is required to produce minimal friction during bending to allow the wire to provide a constant force to the dentition. In the friction state of the bracket model, a regular change in the unloading force such as those observed in Figure 3(b) should be completely hindered as this will cause delays in the formation of bone cells [20, 21] and tooth movement [22]. The study shows the impact of the friction component on the force-deflection response of superelastic NiTi wires upon changing models for the bending. Therefore, the wire and bracket manufacturer should begin finding a new way to reduce the role of friction in orthodontics, so that the constant force behaviour of superelastic NiTi wire can be fully manifested for tooth movement.

It is understood at this juncture that in the three-bracket model, the superelastic NiTi wire experienced greater friction than in the three-point model. Based on Figure 3(b), the intensity of friction at 3.0 mm deflection successfully delayed the unloading force from 2.95 N to 1.34 N. Further care should be paid on this phenomenon as high friction was believed to delay the unloading force further to zero magnitudes, as stated in previous bending studies [23, 24]. As this is the case, it would be important to build a detailed friction database in the near future while using various wire sizes, various bracket materials, and different deflection magnitude. This is important so that the orthodontist can prepare the correct wire bracket combination with regard to the malocclusion status of the patient, thus resulting in a quicker and more relaxed experience of orthodontic care.

Conclusion

The friction intensity at the contact surface gradually increased as a function of deflection magnitude applied to the wire. The wire bent in the bracket model withstands considerably more friction than the point model. The

highest frictional force was obtained when the wire was deflected to 3.0 mm in the bracket model, with the friction magnitude of 2.01 N during loading and 1.61 N during unloading. As soon as the point support was considered, the friction values associated with unloading drastically reduced to 0.25 N. At higher magnitude, friction transformed the constant force trend of superelastic NiTi to a slope.

Acknowledgments

The works have initially been accepted and presented at the MERD'20/AMS'20. The authors thank the financial support provided by Universiti Sains Malaysia under short-term grant 304/PMEKANIK/6315343.

References

- [1] A. Fathallah, T. Hassine, F. Gamaoun, and M. Wali, "Three-dimensional coupling between orthodontic bone remodeling and superelastic behavior of a NiTi wire applied for initial alignment," *Journal of Orofacial Orthopedics*, vol. 82, no. 2, pp. 99–110, 2021.
- [2] W. R. Proffit, H. W. Fields Jr, and D. M. Sarver, *Contemporary Orthodontics*, St. Louis, Mo: Elsevier/Mosby, 2014.
- [3] B. Tran, D. S. Nobes, P. W. Major, J. P. Carey, and D. L. Romanyk, "The three-dimensional mechanical response of orthodontic archwires and brackets in vitro during simulated orthodontic torque," *Journal of the Mechanical Behavior of Biomedical Materials*, vol. 114, pp. 104196, 2021.
- [4] R. Xiao, B. Hou, Q. P. Sun, H. Zhao, and Y. L. Li, "An experimental investigation of the nucleation and the propagation of NiTi martensitic transformation front under impact loading," *International Journal of Impact Engineering*, vol. 140, pp.103559, 2020.
- [5] M. N. Nashrudin, M. F. Razali, and A. S. Mahmud, "Fabrication of step functionally graded NiTi by laser heating," *Journal of Alloys and Compounds*, vol. 828, pp. 154284, 2020.
- [6] H. M. Badawi, R. W. Toogood, J. P. R. Carey, G. Heo, and P. W. Major, "Three-dimensional orthodontic force measurements," *Am. J. Orthod. Dentofac. Orthop.*, vol. 136, no. 4, pp. 518–528, 2009.
- [7] R. Nucera et al., "Influence of bracket-slot design on the forces released by superelastic nickel-titanium alignment wires in different deflection configurations," *Angle Orthod.*, vol. 84, no. 3, pp. 541–7, 2014.

- [8] T. D. Thalman, "Unloading behavior and potential binding of superelastic orthodontic leveling wires," M.Sc dissertation, Dentistry, Saint Louis University, 2008.
- [9] T. Baccetti, L. Franchi, M. Camporesi, E. Defraia, and E. Barbato, "Forces produced by different nonconventional bracket or ligature systems during alignment of apically displaced teeth," *Angle Orthod.*, vol. 79, no. 3, pp. 533–539, 2009.
- [10] J. Q. Whitley and R. P. Kusy, "Influence of interbracket distances on the resistance to sliding of orthodontic appliances," *Am. J. Orthod. Dentofac. Orthop.*, vol. 132, no. 3, pp. 360–372, Sep. 2007.
- [11] F. Auricchio and R. L. Taylor, "Shape-memory alloys: modelling and numerical simulations of the finite-strain superelastic behavior," *Comput. Methods Appl. Mech. Eng.*, vol. 143, no. 1–2, pp. 175–194, Apr. 1997.
- [12] M. F. Razali, A. S. Mahmud, and N. Mokhtar, "Force delivery of NiTi orthodontic arch wire at different magnitude of deflections and temperatures: A finite element study," *J. Mech. Behav. Biomed. Mater.*, vol. 77, pp. 234–241, 2018.
- [13] P. G. Miles, R. J. Weyant, and L. Rustveld, "A clinical trial of Damon 2 vs conventional twin brackets during initial alignment," *Angle Orthod.*, vol. 76, no. 3, pp. 480–485, 2006.
- [14] I. Ben Naceur, A. Charfi, T. Bouraoui, and K. Elleuch, "Finite element modeling of superelastic nickel-titanium orthodontic wires," *J. Biomech.*, vol. 47, no. 15, pp. 3630–8, 2014.
- [15] A. H. Kadarman, S. Shuib, A. Y. Hassan, and M. A. I. A Zahrol, "Thin-walled box beam bending distortion analytical analysis" *Journal of Mechanical Engineering*, vol.14, no. 1, pp. 1-17, 2017.
- [16] A. Manap, M. Faris, S. Shuib, A. Z. Romli, and A. Shokri, "Finite element study of acetabular cup contact region for total hip replacement," *Journal of Mechanical Engineering*, vol 1, pp.71–82, 2017.
- [17] Z. Yusof, A Rasid, and J. Mahmud, "The active strain energy tuning on the parametric resonance of composite plates using finite element method," *Journal of Mechanical Engineering*, vol 15, no. 1, pp.104–119, 2018.
- [18] K. Otsuka and X. Ren, "Physical metallurgy of Ti-Ni-based shape memory alloys," *Prog. Mater. Sci.*, vol. 50, no. 5, pp. 511–678, 2005.
- [19] M. Khairi, N. Aliah, A. Ibrahim, and H. A. Hamid. "Influence of pre-strain on the strain rate response of Ni-Ti shape memory alloy," *Journal of Mechanical Engineering*, vol. 16, no. 2, pp. 157–166, 2019.
- [20] M. T. Cobourne and A. T. DiBiase, *Handbook of Orthodontics*, 2nd ed. Edinburgh, London: Elsevier Health Sciences, 2015. [E-book] Available: Google Books.

- [21] V. Krishnan and Z. E. Davidovitch, “Biological basis of orthodontic tooth movement: A historical perspective,” *Biological Mechanisms of Tooth Movement*, pp. 1–15, 2021.
- [22] V. Krishnan and Z. E. Davidovitch, “Biology of orthodontic tooth movement: the evolution of hypotheses and concepts,” *Biological Mechanisms of Tooth Movement*, pp. 16–31, 2021.
- [23] K. Naziris, N. E. Piro, R. Jäger, F. Schmidt, F. Elkholy, and B. G. Lapatki, “Experimental friction and deflection forces of orthodontic leveling archwires in three-bracket model experiments,” *J. Orofac. Orthop.*, vol. 80, no. 5, pp. 223–235, 2019.
- [24] M. N. Ahmad, A. S. Mahmud, M. F. Razali, and N. Mokhtar, “Binding friction of NiTi archwires at different size and shape in 3-bracket bending configuration,” In *Progress in Engineering Technology II*, pp. 25–32, 2020.